Hindawi
Journal of Advanced Transportation
Volume 2021, Article ID 6611289, 20 pages
https://doi.org/10.1155/2021/6611289

Research Article

Optimizing Train Timetable Based on Departure Time Preference of Passengers for High-Speed Rails

Zhipeng Huang,[1] **Huimin Niu**,[1] **Ruhu Gao**,[1] **Haoyu Fan**,[1] **and Chenglin Liu**[2]

[1]*School of Traffic and Transportation, Lanzhou Jiaotong University, Lanzhou 730070, China*
[2]*School of Information Engineering, Chang'an University, Xi'an 710064, China*

Correspondence should be addressed to Zhipeng Huang; huangzp@mail.lzjtu.cn

Received 28 October 2020; Revised 1 January 2021; Accepted 26 February 2021; Published 10 March 2021

Academic Editor: Roberta Di Pace

Passengers would like to choose the most suitable train based on their travel preferences, expenses, and train timetable in the high-speed railway corridor. Meanwhile, the railway department will constantly adjust the train timetable according to the distribution of passenger flows during a day to achieve the optimal operation cost and energy consumption saving plan. The question is how to meet the differential travel needs of passengers and achieve sustainable goals of service providers. Therefore, it is necessary to design a demand-oriented and environment-friendly high-speed railway timetable. This paper formulates the optimization of train timetable for a given high-speed railway corridor, which is based on the interests of both passengers and transportation department. In particular, a traveling time-space network with virtual departure arc is constructed to analyze generalized travel costs of passengers of each origin-destination (OD), and bilevel programming model is used to optimize the problem. The upper integer programming model regards the minimization of the operating cost, which is simplified to the minimum traveling time of total trains, as the goal. The lower level is a user equilibrium model which arranges each OD passenger flow to different trains. A general advanced metaheuristic algorithm embedded with the Frank–Wolfe method is designed to implement the bilevel programming model. Finally, a real-world numerical experiment is conducted to verify the effectiveness of both the model and the algorithm.

1. Introduction

High-speed railway (HSR) is a high-quality travel service provided by the railway department to the society to meet the spatial displacement needs of passengers and other additional needs within a specific time range. It is worth mentioning that, similar to metro systems, some high-speed railway trains offer no-seat tickets in China. As a representative of safe, fast, comfortable, and sustainable transportation mode, HSR is favored by more and more passengers. For the service provider, the train timetable of HSR is a technical document, which is the foundation of train operation, and integrates the running time of trains in sections and the arrival, departure, or skip-stop time of trains in stations. For passengers, the train timetable is service information of trains released by service providers, which enables them to make reasonable decisions in their journey. Therefore, it is of great practical significance to optimize HSR train timetable.

The optimization of train timetable of HSR, which is based on constraints such as station departure capacity, section carrying capacity, and train safety headway, is to determine the arrival, departure, and skip-stop time of all scheduled trains on a HSR corridor. A perfect train timetable should not only maximize the benefits for transportation enterprises, but also meet the diverse needs of passengers including the traveling cost and departure time preference. Since the 1960s, the train timetable problem (TTP) has been a hot issue in the field of international transportation in the past decades.

From the perspective of service provider, many scholars have concentrated on the optimization of train timetable in terms of train running time, cost, and energy consumption.

As an important evaluating indicator, in some existing literature works, minimizing the total traveling time of all trains is always treated as the objective to optimize train timetable on HSR corridor. The traveling time of train consists of two parts, that is, the running time in sections and the dwelling time at stations. In most HSR corridors, the running time of trains in sections is usually fixed. Therefore, reducing the dwelling time at stations is an effective way to minimize traveling time, as stated by Zhou and Zhong [1] and Abbott et al. [2]. Similarly, Niu and Zhou [3] introduced a variable related to the passenger boarding time range and further established a nonlinear integer programming model to optimize the demand-driven train timetable. Chen and Niu [4] divided traveling process of trains into several continuous events and optimized train timetable based on minimizing the interval of any consecutive events. In addition, a skip-stop scheme and delay time of train at the stations have a great impact on its traveling time. Xu et al. [5] and Heydar et al. [6] set the goal of minimizing total delay time of trains; Wang et al. [7] minimized both the delay time cost of all trains and the number of delayed trains. The ultimate goal of these articles is to optimize train running time.

Transportation enterprises always hope to get the maximum benefit; thus, some scholars have optimized the train timetables to minimize operation costs or maximize operation revenues of trains. From this viewpoint, Cacchiani et al. [8] established a train timetable model with the goal of minimizing operation costs, while Caprara et al. [9] and Cacchiani et al. [10] optimized a train timetable with the goal of maximizing operation revenues. Specifically, Yin et al. [11] established a stochastic programming model to optimize train timetable based on dynamic demand in urban rail transit, with the goal of minimizing train delay time and operator cost. He et al. [12] built an integer programming model to optimize a train timetable with the goal of minimizing the generalized time-space path cost including train running, dwelling, and grade costs.

Reducing the energy consumption of trains is a significant topic, which has been considered in some train timetable optimization studies. Aiming at minimizing energy consumption, Yin et al. [13] established an integer programming model to optimize the train timetable of a subway and designed a heuristic algorithm based on Lagrange relaxation method to solve the original problem. Gupta et al. [14] proposed a two-stage linear train timetable model based on minimum energy consumption of a subway. Ye and Liu [15], Cucala et al. [16], and Watanabe and Koseki [17] also studied train timetable problem with the goal of minimizing energy consumption of trains.

From the perspective of passengers, some papers have studied the train timetable problem with the optimization objective of minimizing the traveling time, waiting time, and transferring time, or the generalized traveling cost.

The most concern of passengers is whether they can get on the train quickly when they arrive at the station. In order to improve the passenger service quality and achieve the people-oriented strategy, a large number of studies have taken minimizing the waiting time of passengers at stations as the goal of train timetable optimization. Aiming at the time-varying OD passenger flow, Niu et al. [18] established a quadratic integer programming model with linear constraints to optimize train timetable problem on a HSR corridor. Hassannayebi et al. [19, 20] established an uneven train timetable model. On this basis, with the goal of minimizing the total waiting time of passengers, Barrena et al. [21] and Canca et al. [22] established a nonlinear integer programming model to optimize train departure and arrival time. Based on the volatility of passenger arrival rate, Shakibayifar et al. [23] established a two-stage stochastic train timetable optimization model. Considering the total traveling time of passengers, Zhou and Zhong [24] established a multiobjective 0-1 mixed-integer programming model to minimize the running time and waiting time of passengers. Shi et al. [25] and Zhang et al. [26] analyzed the characteristics of passenger flows on overcrowded subway lines and established a train timetable optimization model with the goal of minimizing passenger waiting time at all stations.

In the rail transit network, the interval time between two trains arriving at the transfer station continuously is the main factor of determining the waiting time of passengers for transferring. Kang et al. [27] and Guo et al. [28] optimized the train timetable with the goal of minimizing the traveling time and transferring time. Wong et al. [29] established a mixed-integer programming model to optimize a nonperiodic subway network train timetable problem with the goal of minimizing passenger transfer waiting time. Considering the traveling cost of passengers, Chow and Pavlides [30] combined various factors, such as passenger traveling time, waiting time, traveling comfort, and train punctuality to establish a generalized cost function, and built a multiobjective model to minimize it.

The above studies are unilaterally centered on service providers or passengers, but if the interests of both of them can be considered when optimizing the train timetable, it will be a good optimization strategy. Ibarra-Rojas et al. [31] established a biobjective linear integer programming model with the goal of minimizing passengers transferring time and transportation enterprises operating costs to an optimized train timetable. Li et al. [32] considered the collaborative optimization of train carbon emission and passenger traveling time, thus establishing a model of train timetable. Mo et al. [33], Liu et al. [34], and Shen et al. [35] optimized the train timetable by minimizing train energy consumption and passenger waiting time. Tian and Niu [36] aimed at maximizing the number of transfer trains and minimizing the waiting time of passengers and established a biobjective integer programming model to optimize the train timetable. Huang et al. [37] analyzed the relationship between train energy consumption and passenger traveling time and built a nonlinear mixed-integer programming model to optimize a train timetable of subway.

Considering that the interests of service providers and passengers often conflict with each other, for example, reducing the cost of trains may increase the traveling time of passengers, some scholars used bilevel programming method to establish the train timetable model to obtain a

system optimal scheme. Zhu et al. [38] established a bilevel programming model to optimize the urban rail train timetable, in which the upper level optimization is to minimize the generalized cost of passengers, and the lower level is to optimize distribution of passenger flows. Huang and Niu [39] constructed a passenger travel satisfaction function and established a bilevel programming model to study train timetable problem.

Previous studies on TTP rarely considered the difference of passengers' preference for departure time, which is manifested in the fact that passenger flows have obvious peaks and troughs at different time periods of a day. The preference is an important indicator of diversified travel demand of passengers, but few studies have optimized the train timetable driven by travel preference of passengers. It is difficult to ensure the scientificity and rationality of the train timetable which does not consider the passenger's differentiated preference for departure time. Based on previous studies, this paper analyzes the travel behavior of passengers, establishes a generalized cost function for passengers, and uses a bilevel programming to optimize train timetables. The Traffic User Equilibrium (UE) method is used to assign passengers to each train, so as to guide passengers to choose a travel plan reasonably and achieve the goal of minimizing the generalized travel cost.

The main highlights of this paper compared with the existing literature are as follows:

(1) This paper analyzes passengers' preference for departure time and quantifies it by triangular fuzzy method.

(2) This paper constructs a travel time-space network including departure arc, running arc, and dwelling arc. Based on the time preference cost, ticket price cost, and dwelling cost, the impedance functions of various arcs in the space-time network are established, and the travel choice process of passengers is transformed into the path optimization problem in the space-time network.

(3) Considering the Stackelberg Game (SG) relationship between train timetable and passenger flows, a bilevel programming model is constructed, in which the upper level is the optimization of train timetable and the lower level is the assignment of passenger flows.

(4) To improve the efficiency of solution, this paper designs a metaheuristic algorithm of embedded Frank–Wolfe (FW) assignment method to solve the model.

The remainder of this paper is organized as follows. A detailed problem statement is presented in Section 2. Section 3 lists the model assumptions and describes the travel time-space network. In Section 4, a bilevel programming model is developed, and the equivalence between the lower level programming and user equilibrium conditions is proved. Section 5 designs a metaheuristic algorithm. Numerical experiments are tested in Section 6. Finally, Section 7 concludes this paper.

2. Problem Description

This paper focuses on the optimization of train timetable for a bidirectional high-speed railway corridor with m stations, where station 1 and m are the initial and terminal station, respectively, and others are intermediate stations as shown in Figure 1. Up and down trains have their own independent operating tracks including section lines and station arrival-departure tracks, and trains in two directions do not interfere with each other. Considering the relative independence of the up and down trains, this paper only studies the timetable for up trains. In the up direction, all trains depart from the initial station 1, run along the intermediate stations 2, 3, ..., $m-1$, and finally arrive at the terminal station m.

Without loss of generality, we assume that the OD (origin-to-destination) passenger flow matrix on the high-speed railway corridor is predetermined. Meanwhile, there are n trains to be scheduled within the operated time horizon $[T_S, T_E]$, which can be denoted as set $K = \{1, 2, \ldots, n\}$, where the notations T_S and T_E represent the starting and ending timestamps of the scheduled whole operation day.

On the high-speed railway corridor, it is obvious that the OD passenger flow demand is uneven during operated time horizon. Most passengers are used to select the peak period to start their journey. However, due to the restriction of the physical line capacity, it is impossible for all passengers to depart during peak period. Meanwhile, the large passenger flows during peak hours lead to congestion, which further causes passengers to consume extra time and congestion costs in the process of queuing for tickets, waiting for the train, and getting on the train. In response to this situation, this paper designs an uneven train timetable for meeting the traveling preference of different passengers. In addition, when optimizing train timetable, the gamble among different travel decisions should be considered. In this paper, it is proposed to use bilevel programming model to solve our addressed problems. In detail, the train timetable is decided in upper level model, and lower level is a passenger flow assignment problem based on user equilibrium (UE).

In this paper, the relationship between the upper and lower model of the bilevel programming model is shown in Figure 2.

In the upper level, when the running time of trains in the section is fixed, a complete train timetable can be derived. Specifically, firstly, it determines the departure time of the train at initial station (decision 1), then clearly knows the dwelling time at intermediate stations along the railway (decision 2), and finally calculates arrival and departure time of trains at all stations gradually. Train timetable information determined by the upper level will affect the passenger's departure time and traveling time and further affect the passenger's travel impedance (generalized cost), as shown in line ① in Figure 1.

In the lower level, based on UE theory, OD passenger flow demands are loaded onto train operation network determined by the upper level model. In this way, a passenger flow assignment scheme (decision 3) is obtained, which affects train skip-stop pattern of the upper level model and further affects arrival time and departure time of trains

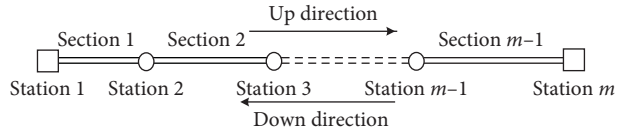

Figure 1: A high-speed railway corridor with double tracks.

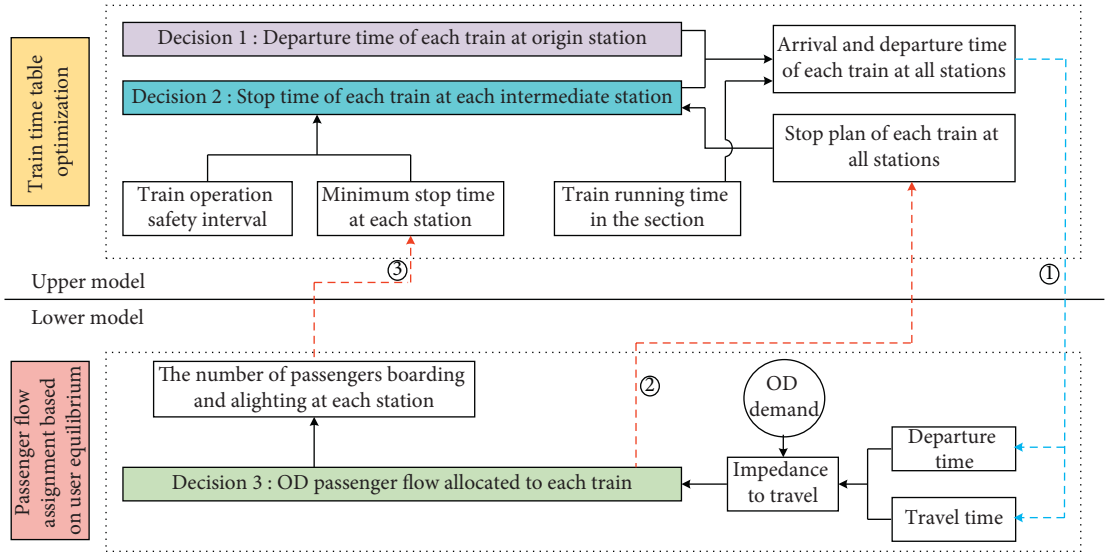

Figure 2: Feedback relationship between upper and lower models.

in the upper level, as shown in the line ② in Figure 1. In addition, based on the scheme of passenger flow assignment, the number of passengers getting on and off at each station can be obtained, as shown in line ③ in Figure 1, which is used to calculate the minimum dwelling time of trains. The arrival and departure time of trains in the upper level model are further affected. As a result, train timetable information in the upper level model and scheme of passenger flow assignment in the lower level model will be adjusted repeatedly until a satisfactory solution is reached.

3. Traveling Time-Space Network (TTSN)

3.1. Overall Notations and Assumptions. In order to simplify the problem and facilitate model construction, several necessary assumptions are detailed as follows:

Assumption 1: All trains run at the same speed on a given high-speed railway corridor. The overtaking operation among different trains will not be considered along the addressed rail corridor.

Assumption 2: The loading capacity of all trains running on the high-speed rail corridor is identical.

Assumption 3: After boarding a train, passengers will not transfer to other trains until arriving at the destination station.

Assumption 4: All passengers are assumed to accurately know generalized cost of each route and will only choose the route with the least cost.

Related indices and parameters in the optimized model are defined as follows:

Sets and indices

$G(N, A)$: Traveling time-space network
N: Node set of network G
A: Arc set of network G
S: Station set
N^{depart}: Departure node set of network G, $N^{\text{depart}} \subseteq N$
N^{arrive}: Arriving node set of network G, $N^{\text{arrive}} \subseteq N$
N^{virtual}: Virtual node set of network G, $N^{\text{virtual}} \subseteq N$
A^{depart}: Departure arc set of network G, $A^{\text{depart}} \subseteq A$
A^{travel}: Traveling arc set of network G, $A^{\text{travel}} \subseteq A$
A^{dwell}: Dwelling arc set of network G, $A^{\text{stop}} \subseteq A$
i, j, r, s: Indices of station, $i, j, r, s \in S$
t, t': Indices of time, $t, t' \in [T_S, T_E]$
a: Indices of arc of network G, $a \in A$
k: Indices of train or path, $k \in K$
(i, t), (j, t'): Indices of time-space node of network G
$(i, t; j, t')$: Indices of time-space arc of network G, $(i, t; j, t') \in A$

Input parameters

q_{rs}: Passenger flow per day from station r to s
Cap_a: Maximum seating capacity of trains on arc a, unit: person
η: The ratio of maximum congestion of trains, $\eta \geq 1$
$h_{i,j}$: Train running time from station i to j, excluding dwelling time and additional start/dwelling time.

$l_{i,j}$: The distance from station i to j
l_a: The length of arc a in network G, $a \in A^{\text{travel}}$
w_a: Passengers' preference degree of departing arc a, $0 \le w_a \le 1$
ε_D: Additional acceleration time
ε_S: Additional deceleration time
$\mu^{\max}$: Maximum dwelling time of trains at stations
$\rho_{\min}^{\text{section}}$: Minimum interval between two consecutive trains at the same section
$\rho_{\min}^{\text{station}}$: Minimum interval between two consecutive trains at the same station
w_{rs}^t: Passengers' preference degree of departing at time t from r to s
g: Unit fee for each passenger per kilometer
α: Cost coefficient of departure time preference
γ: Cost coefficient of waiting time on trains
β_a: Cost coefficient related to passenger flow of arc a
u_{rs}: Minimum number of trains serving OD pairs (r, s)

Auxiliary variables

TA_i^k: Arrival time of train k at station i
TD_i^k: Departure time of train k at station i
$\omega_i^k = 1$ if train k stops at station i and $= 0$ otherwise
$\mu_{i,k}^{\min}$: Minimum dwelling time of train k at station i
$b_{i,k}^{\text{on}}$: The number of passengers boarding on train k at station i
$b_{i,k}^{\text{off}}$: The number of passengers alighting from train k at station i
gc_{rs}^k: Passengers' generalized cost of taking train k from station r to s
c_a: Cost of arc a in network G, $a \in A$
dc_a: Cost of departing arc a in network G, $a \in A^{\text{depart}}$
uc_a: Cost of traveling arc a in network G, $a \in A^{\text{travel}}$
pc_a: Cost of dwelling arc a in network G, $a \in A^{\text{dwell}}$
x_a: Passengers number of arc a in network G, $a = (i, t; j, t')$
$\delta_{rs}^{k,a} = 1$ if train k from station r to s passes through arc a and $= 0$ otherwise

Decision variables

TD_1^k: Departure time of train k at origin station (station 1)
TS_i^k: Dwelling time of train k at station i
f_{rs}^k: The number of passengers taking the train k from station r to s.

3.2. Constructing Traveling Time-Space Network. This section illustrates passenger travel choice process through a simple example. Figure 3(a) shows a high-speed railway corridor containing five stations, where stations 1 and 5 are the initial and terminal stations, respectively. In the research time period, there are 3 trains running on the high-speed railway corridor, and the graphical train timetable is shown in Figure 3(b).

As shown in Figure 4, the whole journey of passengers is divided into three parts in constructed network, which represents the activity of departure, traveling, and dwelling

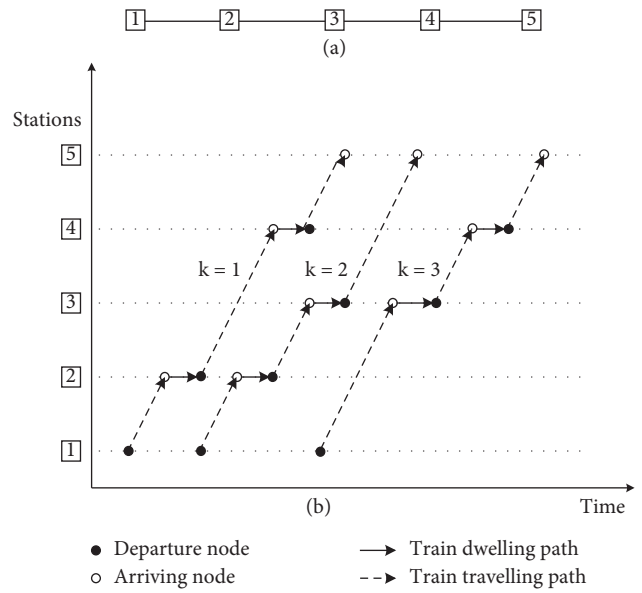

Figure 3: A simple high-speed rail corridor and its graphical train timetable.

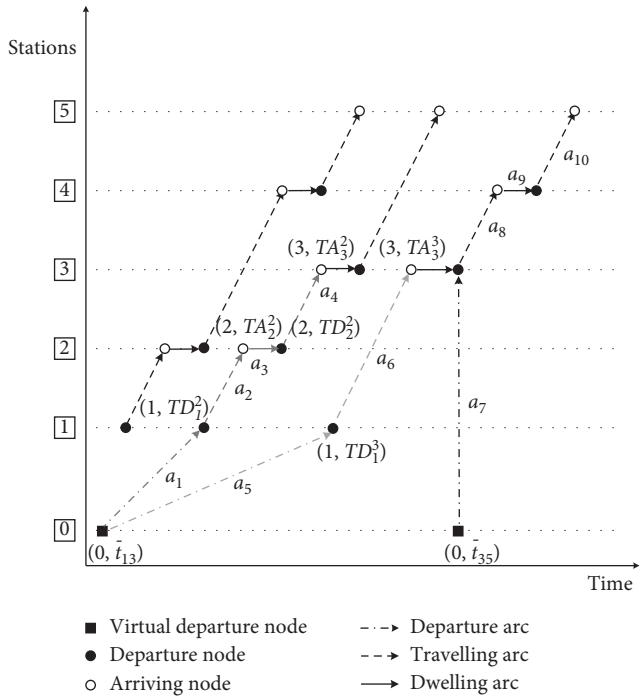

Figure 4: Traveling time-space network for Figure 3(b).

for passengers. For completeness, a virtual station "0" is added in the physical link, which is further extended to a virtual departure node in the constructed network. The set of time-space nodes and arcs in the TTSN are listed in Table 1.

There are three types of nodes, which are departure nodes, arriving nodes, and virtual departure nodes. Among all these nodes, while $i = 0$ and $t = \bar{t}_{rs}$, the symbol $(0, \bar{t}_{rs})$ presents the virtual departure node of the OD pair (r, s), without concrete physical meaning. Besides, all arcs

Table 1: Set of nodes and arcs in TTSN.

Node/Arc	Set
Virtual departure node	$N^{\text{virtual}} = \{(0,t)\|t = \bar{t}_{rs}, \forall r,s \in S\}$
Departure node	$N^{\text{depart}} = \{(i,t)\|i \in S, t = \text{TD}_i^k, \text{when } \omega_i^k = 1, i \neq m\}$
Arriving node	$N^{\text{arrive}} = \{(i,t)\|i \in S, t = \text{TA}_i^k, \text{when } \omega_i^k = 1, i \neq 1\}$
Departure arc	$A^{\text{depart}} = \{(0,t';i,t)\|i < m, t' = \bar{t}_{is}, t = \text{TD}_i^k, \text{when } \omega_i^k \cdot \omega_s^k = 1\}$
Traveling arc	$A^{\text{travel}} = \{(i,t;j,t')\|i,j \in S, t = TD_i^k, t' = \text{TA}_j^k, \text{when } \omega_i^k \cdot \omega_j^k = 1\}$
Dwelling arc	$A^{\text{dwell}} = \{(i,t;i,t + \text{TS}_i^k)\|1 < i < m, t = \text{TA}_i^k, \text{when } \omega_i^k = 1\}$

$(i,t;j,t')$ are time-space ones connecting two time-space nodes (i,t) and (j,t'). For example, the arc a_1 is $a_1(0,\bar{t}_{13};1,\text{TD}_1^2)$. There are three types of arcs in Figure 4, namely, departure arcs, traveling arcs, and dwelling arcs. All these nodes and arcs constitute the TTSN. The process of passenger travel choice, therefore, can be equivalent to determining the optimal path in this time-space network.

Regarding the passenger flow on the TTSN, the sum of passenger flows on each train or each path between any OD pairs (r,s) should equal the total daily passenger demand q_{rs}. For example, in Figure 4, two paths (passengers starting from node 1 and going to node 3), $a_1 \longrightarrow a_2 \longrightarrow a_3 \longrightarrow a_4$ and $a_5 \longrightarrow a_6$, carry two passenger trains on section (1,3), and the corresponding trains on them are trains of $k = 2$ and $k = 3$. Taking f_{13}^2 and f_{13}^3 to represent those passengers on the trains, we can get the equation of $f_{13}^2 + f_{13}^3 = q_{13}$. Likewise, only one path, $a_7 \longrightarrow a_8$, is provided to moving passengers on section (3,4); hence all passenger flows on this path must meet all needs of section (3,4). Then, we get the equation $f_{34}^3 = q_{34}$.

Additionally, the passenger flows on any arc include all paths moving along it in TTSN, and the arc flows equal the sum of all paths' flows. For instance, the arc a_6 in Figure 4 means that the train $k = 3$ runs along section (1,3). Then the passenger flow on arc a_6 can be represented by $f_{13}^3 + f_{14}^3 + f_{15}^3$ since passengers between OD pairs of (1,3), (1,4), and (1,5) can take train of $k = 3$ simultaneously.

3.3. Impedance (Cost) of Each Arc in TTSN. Passengers always want to find the best option before traveling by HSR. It means that the passengers will choose the train with the least impedance (cost) to travel. In TTSN, the cost of each arc is detailed as below.

3.3.1. Impedance of Departure Arc. During a day, passengers have significantly different preferences for departure time. In this paper, the symbol w_{rs}^t is used to represent the preference parameter for the departure arc $(0,\bar{t}_{rs};r,\text{TD}_r^k)$ in OD pair (r,s). It can be quantified by $(T_{rs}^E, T_{rs}^H, T_{rs}^L)$ obtained from data survey, where T_{rs}^E, T_{rs}^L, and T_{rs}^H, respectively, denote the earliest, latest, and most desirable departure time to passengers in OD pair (r,s). As a common method for processing survey data, triangular fuzzy numbers are used to quantify the preferences. The triangular fuzzy number distribution of departure time preference is shown in Figure 5, and its membership function is shown in (1).

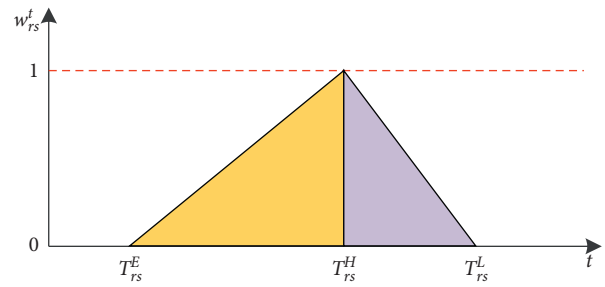

Figure 5: Triangular fuzzy number distribution of departure time preference.

$$w_{rs}^t = \begin{cases} 0, & t \le T_{rs}^E, \\ \dfrac{t - T_{rs}^E}{T_{rs}^H - T_{rs}^E}, & T_{rs}^E < t \le T_{rs}^H, \\ \dfrac{T_{rs}^L - t}{T_{rs}^L - T_{rs}^H}, & T_{rs}^H < t \le T_{rs}^L, \\ 0, & t > T_{rs}^L. \end{cases} \tag{1}$$

For convenience of expression, let $a = (0,\bar{t}_{rs};r,\text{TD}_r^k)$ $w_a = w_{rs}^t$, $a \in A^{\text{depart}}$. w_a is the preference parameter of the departure arc a in TTSN. Based on this, the departure arc cost function, namely, the impedance function, is formulated as

$$\text{dc}_a = \frac{\alpha}{w_a} + \beta_a \cdot \frac{x_a}{\text{Cap}_a}, \quad \forall a \in A^{\text{depart}}, \tag{2}$$

where α/w_a is the passenger's preference costs when choosing departure arc a. It is not difficult to observe that the more the passenger's preference for departure arc a, the less the preference cost they pay; $\beta_a \cdot x_a/\text{Cap}_a$is the passenger flow-related costs on the departure arc$a$, and it can be quantified by the input coefficient β_a. When the passenger flow x_a loaded on the departure arc a increases, the impedance increases accordingly.

3.3.2. Impedance of Traveling Arc. Traveling arc cost function can be constructed as

$$uc_a = g \cdot l_a + \beta_a \cdot \frac{x_a}{\mathrm{Cap}_a}, \quad \forall a \in A^{\mathrm{travel}}, \tag{3}$$

where $g \cdot l_a$ is the ticket price cost by passenger on traveling arc a. Similar to the departure arc, $\beta_a \cdot x_a/\mathrm{Cap}_a$ indicates that the cost of traveling arc increases with the increase of passenger flows.

3.3.3. Impedance of Dwelling Arc. When a train dwells at an intermediate station, the waiting time of passengers at the station will increase, and the time can be quantified by waiting time cost. It can be written as

$$pc_a = \gamma \cdot \left(\mathrm{TS}_i^k + \varepsilon_S + \varepsilon_D\right) + \beta_a \cdot \frac{x_a}{\mathrm{Cap}_a}, \quad \forall a \in A^{\mathrm{dwell}}. \tag{4}$$

The additional acceleration and deceleration times should be considered once the train dwells at a station. Therefore, $\gamma \cdot (\mathrm{TS}_i^k + \varepsilon_S + \varepsilon_D)$ is the waiting time cost of passengers on the dwelling arc.

For simplicity of expression, we use c_a to represent the impedance of any arc a in the TTSN. The impedance function is shown as

$$c_a = \begin{cases} \mathrm{dc}_a, & a \in A^{\mathrm{depart}}, \\ uc_a, & a \in A^{\mathrm{travel}}, \\ pc_a, & a \in A^{\mathrm{dwell}}, \end{cases} \quad \forall a \in A. \tag{5}$$

In summary, for any passengers of OD pair (r, s), from the boarding station r to the alighting station s, passengers will travel through the above various arcs. The sum of the costs paid on all arcs is called generalized cost, also known as route impedance, and is shown in

$$\mathrm{gc}_{rs}^k = \sum_{a \in A} c_a \cdot \delta_{rs}^{k,a}. \tag{6}$$

4. Model Formulation

In this paper, a bilevel programming model is developed to solve the problem, in which the upper level model determines the train timetable, and the lower level model assigns the OD passenger flows on different trains.

4.1. Upper Level Programming Model

4.1.1. Objective Function. This paper aims to optimize the train timetable under the condition that the number and type of trains are determined. Thus, the total cost of train operations is fixed. The number of skip-stop patterns and the dwelling time of trains at the intermediate stations will result in different total traveling time. Therefore, the upper level model is simplified to minimize the total traveling time of all trains, including section running time and station dwelling time, as shown in

$$\min Z_{\mathrm{upper}} = \sum_{k \in K} \left(\mathrm{TA}_m^k - \mathrm{TD}_1^k\right), \tag{7}$$

where $\mathrm{TA}_m^k - \mathrm{TD}_1^k$ is the traveling time of the train k between the initial station 1 and the terminal station m.

4.1.2. Train Arrival and Departure Time Constraints. The arrival time of the train $k$at the station i can be calculated from the departure time TD_{i-1}^k, the running time in the section $h_{i-1,i}$ and the additional acceleration and deceleration time of the train k at the front station $i-1$ $(i > 1)$, as shown in

$$\mathrm{TA}_i^k = \mathrm{TD}_{i-1}^k + h_{i-1,i} + \varepsilon_D \cdot \omega_{i-1}^k + \varepsilon_S \cdot \omega_i^k, \quad \forall i > 1, k. \tag{8}$$

The arrival time TD_i^k of the train k at the station i can be calculated by the arrival time TA_i^k and the dwelling time TS_i^k, as shown in

$$\mathrm{TD}_i^k = \mathrm{TA}_i^k + \mathrm{TS}_i^k, \quad \forall i, k. \tag{9}$$

4.1.3. Constraint on Safety Interval of Train. After the train k departs from station i, there must be a station safety interval $\rho_{\min}^{\mathrm{station}}$ to ensure that it is safe for adjacent train $k+1$ to arrive at station i as shown in (10). In addition, there must be a minimum section safety interval time to ensure that adjacent trains are safe in the section as shown in (11).

$$\mathrm{TA}_i^{k+1} - \mathrm{TD}_i^k \geq \rho_{\min}^{\mathrm{station}}, \quad \forall i, k, \tag{10}$$

$$\mathrm{TD}_i^{k+1} - \mathrm{TD}_i^k \geq \rho_{\min}^{\mathrm{section}}, \quad \forall i, k. \tag{11}$$

4.1.4. Dwelling Time Constraints. The minimum dwelling time $\mu_{i,k}^{\min}$ is related to the number of passengers boarding and alighting from the train at the station i, as shown in (12), where ϕ is the average time of a passenger boarding or alighting from trains. The number of passengers boarding the train $b_{i,k}^{\mathrm{on}}$ and the number of passengers alighting from the train $b_{i,k}^{\mathrm{off}}$ are calculated from the passenger flow assignment in the lower level model, as shown in (13) and (14). In summary, the dwelling time of trains at intermediate stations along the HSR corridor should satisfy (15).

$$\mu_{i,k}^{\min} = \phi \cdot \left(b_{i,k}^{\mathrm{on}} + b_{i,k}^{\mathrm{off}}\right), \quad \forall i, k, \tag{12}$$

$$b_{i,k}^{\mathrm{on}} = \sum_{j > i} f_{ij}^k, \quad \forall i, k, \tag{13}$$

$$b_{i,k}^{\mathrm{off}} = \sum_{s < i} f_{si}^k, \quad \forall i, k, \tag{14}$$

$$\begin{cases} \mu_{\min}^{i,k} \leq \mathrm{TS}_i^k \leq \mu_{\max}, & \text{if } \omega_i^k = 1, \\ \mathrm{TS}_i^k = 0, & \text{if } \omega_i^k = 0, \end{cases} \quad \forall i, k. \tag{15}$$

4.1.5. Train Service Capacity Constraint. If a train k dwells at both stations r and s, that is, $\omega_r^k \cdot \omega_s^k = 1$, passengers departing from station r and arriving at station s may have a chance to board the train. The number of trains serving OD pair (r, s) should satisfy the below constraint.

$$\sum_{k} \omega_r^k \cdot \omega_s^k \geq u_{rs}. \tag{16}$$

4.2. Lower Level Programming

4.2.1. Objective Function

$$\min Z_{\text{lower}} = \sum_{a \in A} \int_0^{x_a} c_a(\varphi) \mathrm{d}\varphi. \tag{17}$$

The lower level model is a passenger flow assignment model based on UE theory; its objective function is shown in (17). The objective function itself has no intuitive economic meaning. It is just the best way to find the optimal passenger flow assignment scheme with the minimum and equal generalized travel cost of the same OD pair in TTSN, and mathematical proof will be given later.

4.2.2. Constraints

$$\sum_{k \in K} f_{rs}^k = q_{rs}, \quad \forall r, s, \tag{18}$$

$$f_{rs}^k \geq 0, \quad \forall r, s, k, \tag{19}$$

$$x_a = \sum_{k \in K} \sum_{r \in S} \sum_{s \in S} f_{rs}^k \cdot \delta_{rs}^{k,a}, \quad \forall k, r, s, \tag{20}$$

$$x_a \leq \eta \cdot \text{Cap}_a, \quad \forall a. \tag{21}$$

Equation (18) is passenger flow conservation constraint; (19) is passenger flow nonnegative constraint; (20) indicates that the arc flow x_a is superimposed by all the path flows containing the arc a. Equation (21) is a capacity constraint, which means that the accumulated passenger flow on arc a cannot exceed its service capacity.

4.2.3. Proof of Equivalence between Low-Level Programming Model and Wardrop First Principle. The lower-level programming model constructed is a passenger flow equilibrium assignment model with arc capacity constraints (21). Due to capacity restrictions, arc a also adds a cost penalty. Let u_a denote the penalty cost on arc a, and it satisfies

$$\begin{cases} u_a = 0, & \text{if } x_a < \eta \cdot \text{Cap}_a, \\ u_a \geq 0, & \text{if } x_a = \eta \cdot \text{Cap}_a, \end{cases} \tag{22}$$

λ_{rs} is the minimum generalized cost of OD pair (r, s); according to the user equilibrium conditions of Wardrop, the formula is as follows:

$$\begin{cases} \sum_{a \in A} (c_a + u_a) \cdot \delta_{rs}^{k,a} = \lambda_{rs}, & \text{if } f_{rs}^k > 0, \\ \sum_{a \in A} (c_a + u_a) \cdot \delta_{rs}^{k,a} \geq \lambda_{rs}, & \text{if } f_{rs}^k = 0. \end{cases} \tag{23}$$

Through the above analysis, the lower level model is a minimum problem with capacity constraints. According to the nonlinear programming theory, the lower level model must be modified firstly. The Lagrange multipliers λ_{rs} and τ_a are introduced for passenger flow conservation and capacity constraints, and the original model is mathematically described with a Lagrangian function, as shown in

$$\begin{aligned} L(f, \lambda, \tau) = & \sum_{a \in A} \int_0^{x_a} c_a(\varphi) \mathrm{d}\varphi + \sum_{r,s \in S} \lambda_{rs} \\ & \cdot \left(q_{rs} - \sum_{k \in K} f_{rs}^k \right) + \sum_{a \in A} \tau_a \\ & \cdot \left(\eta \cdot \text{Cap}_a - \sum_{r,s \in S} \sum_{k \in K} f_{rs}^k \cdot \delta_{rs}^{k,a} \right). \end{aligned} \tag{24}$$

In order to obtain the stagnation point of the lower level model, (25) must be satisfied:

$$\begin{cases} & \min L(f, \lambda, \tau), \\ f_{rs}^k \geq 0, & \forall k \in K, r, s \in S, \\ \tau_a \cdot \left(\eta \cdot \text{Cap}_a - \sum_{r,s \in S} \sum_{k \in K} f_{rs}^k \cdot \delta_{rs}^{k,a} \right) = 0, & \forall a \in A, \\ \eta \cdot \text{Cap}_a - \sum_{r,s \in S} \sum_{k \in K} f_{rs}^k \cdot \delta_{rs}^{k,a} \geq 0, & \forall a \in A, \\ \tau_a \leq 0, & \forall a \in A. \end{cases} \tag{25}$$

The first-order condition of (25) is shown in

$$\begin{cases} f_{rs}^k \cdot \dfrac{\partial L}{\partial f_{rs}^k} = 0, \dfrac{\partial L}{\partial f_{rs}^k} \geq 0, & \forall r, s \in S, k \in K, \\ \dfrac{\partial L}{\partial \lambda_{rs}} = 0, & \forall r, s \in S, \\ \tau_a \cdot \left(\eta \cdot \text{Cap}_a - \sum_{r,s \in S} \sum_{k \in K} f_{rs}^k \cdot \delta_{rs}^{k,a} \right) = 0, & \forall a \in A, \\ \eta \cdot \text{Cap}_a - \sum_{r,s \in S} \sum_{k \in K} f_{rs}^k \cdot \delta_{rs}^{k,a} \geq 0, & \forall a \in A, \\ \tau_a \leq 0, & \forall a \in A. \end{cases} \tag{26}$$

To find the first-order derivatives $(\partial L / \partial f_{rs}^k)$ and $(\partial L / \partial \lambda_{rs})$of $L(f, \lambda, \tau)$, (26) can be transformed into the following formula:

$$\begin{cases} f_{rs}^{k} \cdot \left(\sum_{a \in A} c_a \cdot \delta_{rs}^{k,a} - \lambda_{rs} - \sum_{a \in A} \tau_a \cdot \delta_{rs}^{k,a} \right) = 0, & \forall k \in K, r, s \in S, \\ \sum_{a \in A} c_a \cdot \delta_{rs}^{k,a} - \lambda_{rs} - \sum_{a \in A} \tau_a \cdot \delta_{rs}^{k,a} \geq 0, & \forall k \in K, r, s \in S, \\ q_{rs} = \sum_{k \in K} f_{rs}^{k}, & \forall r, s \in S, \\ \tau_a \cdot \left(\eta \cdot \mathrm{Cap}_a - \sum_{r,s \in S} \sum_{k \in K} f_{rs}^{k} \cdot \delta_{rs}^{k,a} \right) = 0, & \forall a \in A, \\ \eta \cdot \mathrm{Cap}_a - \sum_{r,s \in S} \sum_{k \in K} f_{rs}^{k} \cdot \delta_{rs}^{k,a} \geq 0, & \forall a \in A, \\ \tau_a \leq 0, & \forall a \in A. \end{cases} \tag{27}$$

From (27), the equilibrium condition can be obtained as

$$\begin{cases} \sum_{a \in A} c_a \cdot \delta_{rs}^{k,a} - \sum_{a \in A} \tau_a \cdot \delta_{rs}^{k,a} = \lambda_{rs}, & \text{if } f_{rs}^{k} > 0, \\ \sum_{a \in A} c_a \cdot \delta_{rs}^{k,a} - \sum_{a \in A} \tau_a \cdot \delta_{rs}^{k,a} \geq \lambda_{rs}, & \text{if } f_{rs}^{k} = 0, \end{cases} \quad \forall a \in A. \tag{28}$$

When $\sum_{r,s \in S} \sum_{k \in K} f_{rs}^{k} \cdot \delta_{rs}^{k,a} < \eta \cdot \mathrm{Cap}_a$, then $\tau_a = 0$; when $\sum_{r,s \in S} \sum_{k \in K} f_{rs}^{k} \cdot \delta_{rs}^{k,a} = \eta \cdot \mathrm{Cap}_a$, then $\tau_a \leq 0$. From (23), we can see that $u_a = -\tau_a$; that is, the penalty cost u_a of arc a corresponds to its Lagrange multiplier τ_a. The Lagrangian multiplier λ_{rs} of passenger flow conservation constraint is the minimum generalized travel cost of OD pair (r, s). Therefore, (28) is equivalent to (23), and the proof is complete.

5. Implementations of Algorithm

The developed model in the paper is a bilevel programming model. It has proved to be a nondeterministic polynomial (NP-hard) problem (Brimberg et al. [40], Sun et al. [41]), which is difficult to solve by general gradient-based optimization approach or commercial optimization solver. The genetic algorithm (GA) is exploited to solve the upper level programming model, and the Frank–Wolfe algorithm is applied to determine the lower level programming model.

5.1. Genetic Algorithm

5.1.1. Chromosome Coding. The chromosome is coded by integers and consists of n gene segments, representing n trains, as shown in Figure 6. Each gene fragment has the same structure, and it has $m - 1$ gene positions. In particular, the first position represents the departure time of train k at the initial station 1, and the $2 \sim m - 1$ position represents the dwelling time of the train at station $2 \sim m - 1$, respectively.

We will take a simple example to illustrate the coding rules of the above chromosomes. As shown in Figure 7, the train k departs from initial station at the 360th minute (6 : 00 am), the dwelling times are 6 min, 0 min, and 3 min at stations 2, 3, and 4, respectively. The corresponding gene position is 360, 6, 0, 3 for the train k. Furthermore, the departure and arrival time of train k at all stations can be deduced from the numbers of the above 4 gene positions according to (8) and (9).

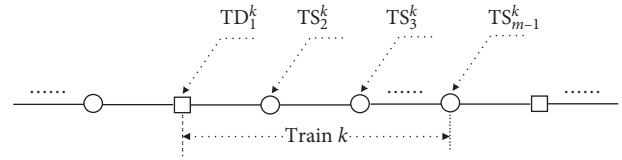

Figure 6: Chromosome structure.

5.1.2. Genetic Operation. Selection operation: When performing a selection operation, the best individual of this generation is retained to enter the next operation according to the degree of fitness, and the remaining individuals are randomly selected according to roulette. The detailed steps are as follows: Firstly, calculate the total fitness of all chromosomes ℓ_b in the population according to (29); then, compute the probability of chromosome being selected according to (30); finally, generate a random number $\kappa_{\mathrm{rand}} \in [0, 1]$, and select the chromosome if it satisfies (31).

$$\mathrm{fitness}_{\mathrm{sum}} = \sum_{b=1}^{P_{\mathrm{size}}} \mathrm{fitness}(\ell_b), \tag{29}$$

$$p(\ell_b) = \frac{\mathrm{fitness}(\ell_b)}{\mathrm{fitness}_{\mathrm{sum}}}, \tag{30}$$

$$\begin{aligned} p(\ell_1) + p(\ell_2) + \cdots + p(\ell_{b-1}) &\leq \kappa_{\mathrm{rand}} \\ &\leq p(\ell_1) + p(\ell_2) + \cdots + p(\ell_b). \end{aligned} \tag{31}$$

Crossover operation: We use a bipoint crossover operation; that is, we randomly select two crossover points and then generate a random number $\zeta_{\mathrm{rand}} \in [0, 1]$. If ζ_{rand} is less than the preset crossover probability P_c, then we exchange the gene sequences of the two selected parent chromosomes between two crossover points. The detailed procedure of crossover operation is shown in Figure 8.

Mutation operation: According to the characteristics of chromosome coding, this paper uses three mutation probabilities, P_m^1, P_m^2, and P_m^3, to perform mutation operations as follows:

(1) If the selected gene position is $\mathrm{TS}_i^k \in [\mu_{i,k}^{\min}, \mu^{\max}]$ and $\xi_{\mathrm{rand}} < P_m^1$, then set the value of gene position TS_i^k to 0.

(2) If the selected gene position is $\mathrm{TS}_i^k = 0$ and $\xi_{\mathrm{rand}} < P_m^2$, then set the value of gene position TS_i^k to an integer between $\mu_{i,k}^{\min}$ and $\mu^{\max}$.

(3) If the selected gene position is TD_i^k and $\xi_{\mathrm{rand}} < P_m^3$, then an integer is randomly selected to replace it within the departure time range.

An example of the above mutation operation is shown in Figure 9. Station 2 was randomly selected as the mutation point, and the value TS_2^k changes from 6 to 0.

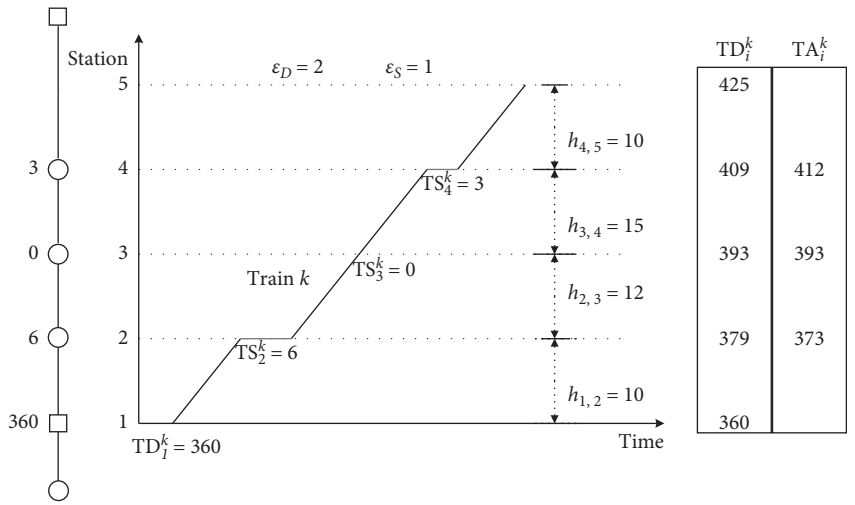

Figure 7: Code rules for chromosomes.

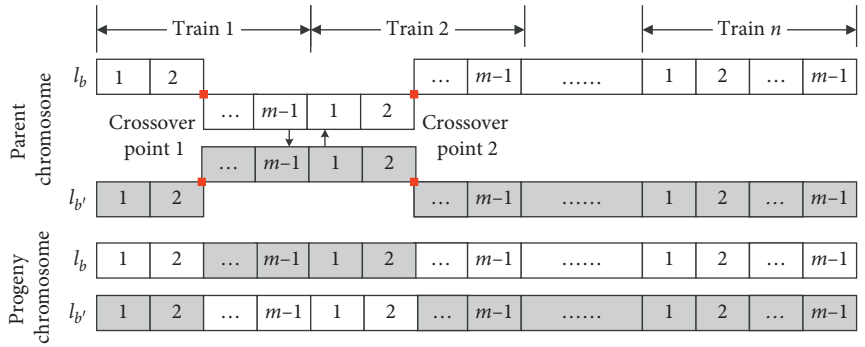

Figure 8: A schematic diagram of the chromosome two-point crossover operator.

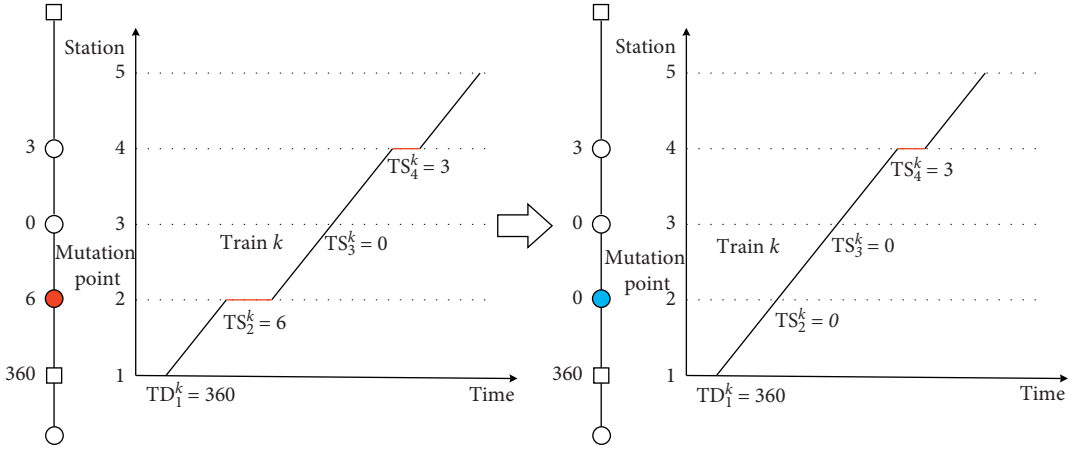

Figure 9: Mutation operation.

Since the trains' departure time and dwelling time are affected by the station interval time and train departure interval time, some chromosomes after initialization and cross-mutation will lose their generality and need to be adjusted.

(1) *Adjustment method of station safety interval.* For example, at station 3, the difference of the arrival time of train $k+1$ and the departure time of train $k$conflicts with the station safety interval; that is, $TA_3^{k+1} - TD_3^k < \rho_{\min}^{\text{station}}$; then, TA_3^{k+1} needs to be adjusted as $TA_3^{k+1'}$, $TA_3^{k+1'} = TA_3^{k+1} + \nabla$. The notation ∇ denotes the adjustment amount, $\nabla = \rho_{\min}^{\text{station}} - (TA_3^{k+1} - TD_3^k)$. Meanwhile, the arrival and departure time of the train $k+1$ at all other stations are increased by ∇, as shown in Figure 10:

(2) *Adjustment method of section interval.* For example, at station 3, for the adjacent trains$k$ and $k+1$, if

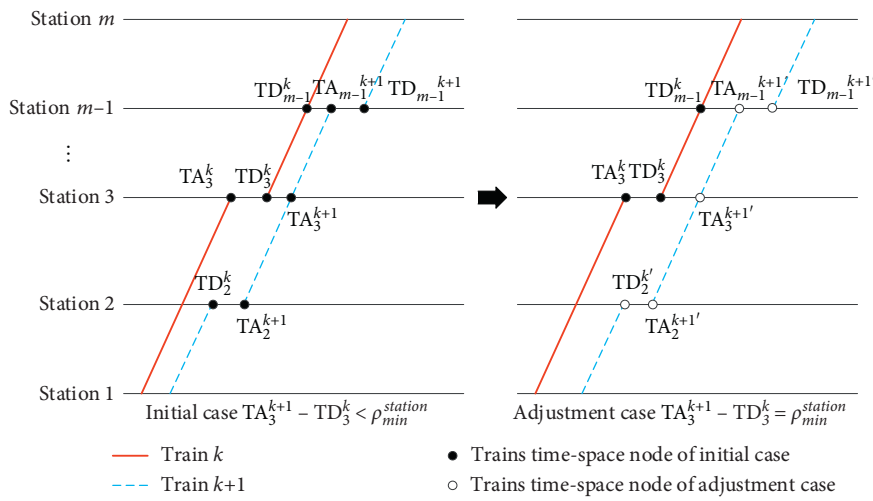

Figure 10: Adjustment method of station interval.

$TD_3^{k+1} - TD_3^k < \rho_{\min}^{\text{section}}$, then TD_3^{k+1} need to be adjusted as $TD_3^{k+1'}$, $TD_3^{k+1'} = TD_3^{k+1} + \nabla$. The symbol ∇ represents the adjusted amount, $\nabla = \rho_{\min}^{\text{section}} - (TD_3^{k+1} - TD_3^k)$. Meanwhile, the arrival and departure time of train $k+1$ are increased by ∇ from station 3 to terminal station$m$, as shown in Figure 11.

5.2. Frank–Wolfe Algorithm. We fix the current train timetable $\Omega^{(o)}$ determined by the upper level programming and then solve the lower level programming by Frank–Wolfe algorithm to obtain x_a which conforms to the principle of Wardrop user equilibrium. The specific processes are listed as follows:

(0) Initialize: Set the impedance $c_a(\cdot) = c_a(0)$ for all arcs in TTSN. Calculate the generalized cost $gc_{rs}^k(0)$ by (6). The passenger flow demands that $\{q_{rs}\}$ is allocated to the path with the smallest generalized cost by "all-or-nothing" method; then, the flow of each arc $\{x_a^{(1)}\}$ is obtained. Set iteration $o = 1$.

(1) Update the impedance of all arcs in TTSN.

(2) Search the iteration direction: According to $\{c_a(x_a)\}$, $\{q_{rs}\}$ is allocated to the path with the smallest generalized cost by using the "all-or-nothing" method to obtain a set of additional arc flows $\{y_a^{(o)}\}$.

(3) Calculate the length of iteration step: Use the dichotomy approach to find ξ which satisfies the formula

$$\sum_a \left(y_a^{(o)} - x_a^{(o)}\right) \cdot c_a\left[x_a^{(o)} + \xi \cdot \left(y_a^{(o)} - x_a^{(o)}\right)\right] = 0. \quad (32)$$

(4) Update the cumulative flow of each arc through the recurrence formula

$$x_a^{(o+1)} = x_a^{(o)} + \xi \cdot \left(y_a^{(o)} - x_a^{(o)}\right), \quad \forall a. \quad (33)$$

(5) If the convergence criterion of (34) is satisfied, terminate the algorithm; otherwise, set $o = o + 1$ and go to Step (1).

$$\frac{\sqrt{\sum_a \left(x_a^{(o+1)} - x_a^{(o)}\right)^2}}{\sum_a x_a^{(o)}} < \Delta, \quad (34)$$

where Δ is the predetermined allowed deviation.

5.3. The Genetic Algorithm Process of the Nested Frank–Wolfe Method

Step 1: Initialize.

Step 1.1: Initialize the maximum iteration Ge, crossover probability P_c, and mutation probability P_m^1, P_m^2, and P_m^3; set the loop variable $\varsigma_1 = 0$.
Step 1.2: Assign an initial value ϑ to the auxiliary variable $\mu_{i,k}^{\min}$, and randomly generate an initial feasible solution $\left\{TD_1^k, TS_i^k | 1 < i < m, i \in S, k \in K\right\}$ according to the above chromosome coding rules.
Step 1.3: According to (8) and (9), generate the train timetable $\left\{TD_i^k, TA_i^k | i \in S, k \in K\right\}$.
Step 1.4: If the current chromosome satisfies (8)~(11), then set the loop variable $\varsigma_1 = \varsigma_1 + 1$ and go to Step 1.5; otherwise, return to Step 1.2 to regenerate a chromosome.
Step 1.5: If $\varsigma_1 = P_{\text{size}}$, the initial population is obtained, and then go to Step 1.6; otherwise, go to Step 1.2.
Step 1.6: Set the iteration $\eta = 0$ and go to Step 2.

Step 2: Calculate the fitness of each chromosome in the initial population

Step 2.1: According to the coding scheme of each chromosome in the population, update the skip-stop pattern $\{\omega_i^k | 1 < i < m, i \in S, k \in K\}$ of the train k at the intermediate station and the train timetable $\left\{TD_i^k, TA_i^k | i \in S, k \in K\right\}$.
Step 2.2: Set the loop variable $\varsigma_2 = 0$.
Step 2.3: For the current chromosome, use the Frank–Wolfe algorithm to solve the lower level

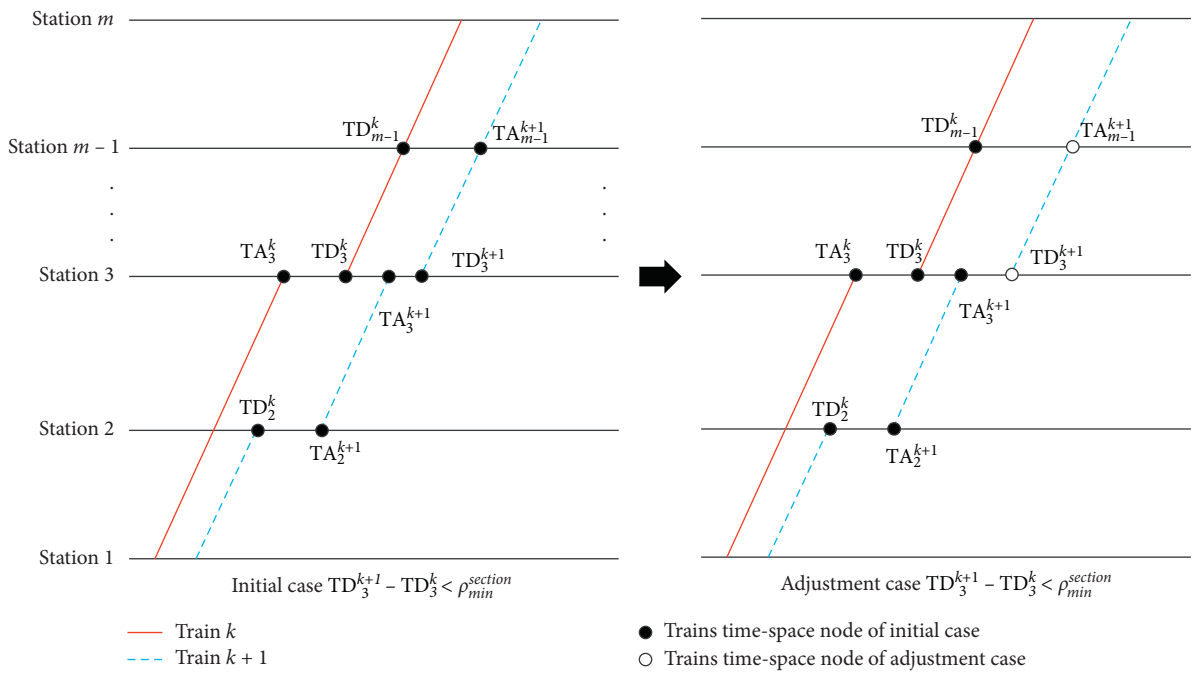

Figure 11: Adjustment method of section interval.

planning, and obtain the allocation results $\{f^k_{ij} | i, j \in S, k \in K\}$ of each OD pair.

Step 2.4: According to (13) and (14), calculate the number of boarding passengers $b^{on}_{i,k}$ and alighting passengers $b^{off}_{i,k}$ at the station$i$, and then calculate the value of the parameter $\mu^{min}_{i,k}$ under the current distribution result according to (12). If $\mu^{min}_{i,k} < \vartheta$, put the corresponding chromosome into the mating pool, set $\varsigma_2 = \varsigma_2 + 1$, and go to Step 2.5; otherwise, adjust TS^k_i and TD^k_i according to the chromosome adjustment method designed above, and go to Step 2.3.

Step 2.5: If $\varsigma_2 = P_{size}$, go to Step 2.6; otherwise, go to Step 2.3.

Step 2.6: Calculate the fitness of each chromosome for the current population.

Step 3: Update the population using genetic operations.

Step 3.1: Use the genetic operations to perform selection operations, crossover operations, and mutation operations to obtain a new population, and set the iterations $\eta = \eta + 1$.

Step 3.2: Check whether all chromosomes in the current population satisfy (10)~(11), and set the loop variable $\varsigma_3 = 0$.

Step 3.3: Check whether each gene value of the current chromosome satisfies (10)~(11); if so, put the current chromosome into the mating pool, set $\varsigma_3 = \varsigma_3 + 1$, and go to Step 3.4; otherwise, go to Step 4 to repair the chromosome to ensure the feasibility of the population.

Step 3.4: If $\varsigma_3 = P_{size}$, go to Step 5; otherwise, go to Step 3.2.

Step 4: Repair chromosome.

Step 4.1: Set loop variable $\varsigma_4 = 0$.

Step 4.2: According to the current chromosome value, decode the chromosome to get the timetable $\{TA^k_i, TD^k_i | i \in S, k \in K\}$.

Step 4.3: Check whether the trains k and $k+1$ at stations satisfy (11) in the current timetable. If they satisfy the requirements, go to Step 4.5; if not, go to Step 4.6.

Step 4.4: Set $TA^{k+1}_s = TA^{k+1}_s + \nabla$, $TD^{k+1}_s = TD^{k+1}_s + \nabla$, $j \le s \le m$, and $\omega^{k+1}_{j'} = 0$, $j < j' < i$, $\nabla = \rho^{station}_{min} - (TA^{k+1}_i - TD^k_i)$; go to Step 4.6.

Step 4.5: Check whether the trains k and $k+1$ at stations satisfy (12) in the current timetable. If they satisfy the requirements, go to Step 3; if not, go to Step 4.6.

Step 4.6: Set $TA^{k+1}_s = TA^{k+1}_s + \nabla$, $TD^{k+1}_s = TD^{k+1}_s + \nabla$, $i \le s \le m$, $\nabla = \rho^{station}_{min} - (TD^{k+1}_i - TD^k_i)$, and go to Step 3.

Step 5: Judgment of terminate condition: If the number of iterations η is more than the maximum iteration Ge, go to Step 6; otherwise, go to Step 2.

Step 6: Output the result.

Output the most adaptive decision variables $\{TD^k_1, TS^k_i | 1 < i < m, i \in S, k \in K\}$ in the current generation, and calculate the timetable $\{TD^k_i, TA^k_i | i \in S, k \in K\}$ and the results of flow assignment in the lower layer model.

6. Numerical Experiments

6.1. Input Parameter Setting. In this section, the proposed models and algorithms will be demonstrated by a real-world example based on the Lanzhou-Xi'an high-speed railway

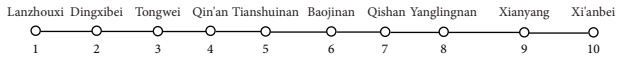

Figure 12: Schematic diagram of Lanzhou-Xi'an high-speed railway corridor.

Table 2: The values of parameters $h_{i,i+1}$ and $l_{i,i+1}$ (min, km).

i	1	2	3	4	5	6	7	8	9
$h_{i,i+1}$	26.9	20.4	14.3	10.6	36.8	9.7	10.7	15.7	9.0
$l_{i,i+1}$	103	78	55	41	141	37	41	60	35

Table 3: The values of other input parameters.

Parameters	Values
n	65 trains
α	2.5
ε_S	1 min
ε_D	2 min
$\mu^{\max}$	6 min
γ	2 CNY/min
$\rho_{\min}^{\text{section}}$	3 min
$\rho_{\min}^{\text{station}}$	2 min
ϕ	0.36 sec
Δ	0.001
β_a	5, $\forall a \in A^{\text{depart}}$
β_a	0.4, $\forall a \in A^{\text{travel}}$
β_a	0.5, $\forall a \in A^{\text{dwell}}$
g	0.3 CNY/person/km
Cap_a	600 persons, $\forall a \in A$

Table 4: Daily average OD passenger flow data of Lanzhou-Xi'an high-speed railway corridor.

Station	Station j								
i	2	3	4	5	6	7	8	9	10
1	2247	674	1124	3596	3371	1124	899	1124	3820
2	—	300	262	449	300	112	112	150	562
3	—	—	75	112	75	37	37	75	150
4	—	—	—	150	75	37	37	112	150
5	—	—	—	—	749	75	112	187	2622
6	—	—	—	—	—	375	562	562	1498
7	—	—	—	—	—	—	187	187	375
8	—	—	—	—	—	—	—	187	749
9	—	—	—	—	—	—	—	—	187
total	2247	974	1461	4307	4570	1760	1946	2584	29963

corridor in China, which consists of 10 stations and 9 sections, as shown in Figure 12. For convenience, the stations are numbered as 1, 2, . . ., 10 along the up direction. The distance and train running time of each section are listed in Table 2. Other input parameters are shown in Tables 3 and 4. The passenger demand for each OD pair within operating period can be found in Table 5.

In addition, the necessary parameters associated with the developed metaheuristic algorithm should be carefully specified. We set population size in the genetic algorithm to $P_{\text{size}} = 100$, crossover probability to $P_c = 0.8$, $P_m^1 = 0.07$,

Table 5: The optimized departure/arrival time on origin/terminal station for each train.

Train no.	Departure time	Arrival time
1	6:17	9:26
2	6:33	9:44
3	6:41	9:47
4	6:50	10:08
5	7:17	10:34
6	7:45	10:37
7	7:48	10:55
8	8:14	10:58
9	8:17	11:8
10	8:20	11:32
11	8:34	11:39
12	8:40	11:49
13	8:57	11:55
14	9:06	12:06
15	9:17	12:27
16	9:39	12:30
17	9:42	12:42
18	10:07	12:52
19	10:10	13:28
20	10:28	13:43
21	10:52	13:50
22	10:55	14:17
23	11:22	14:20
24	11:34	14:52
25	12:04	15:03
26	12:15	15:6
27	12:19	15:11
28	12:28	15:41
29	12:51	15:49
30	12:54	15:57
31	13:05	16:21
32	13:19	16:34
33	13:45	16:37
34	13:53	16:58
35	14:01	17:23
36	14:24	17:27
37	14:41	17:35
38	14:52	17:48
39	14:55	18:03
40	15:16	18:06
41	15:19	18:25
42	15:27	18:37
43	15:54	18:49
44	16:05	19:13
45	16:21	19:31
46	16:37	19:46
47	16:42	19:49
48	16:57	19:57
49	17:05	20:17
50	17:10	20:25
51	17:29	20:28
52	17:39	20:31
53	17:42	20:52
54	17:57	21:17
55	18:34	21:20
56	18:43	21:37
57	18:46	22:06
58	19:11	22:24
59	19:20	22:27

Table 5: Continued.

Train no.	Departure time	Arrival time
60	19 : 33	22 : 46
61	19 : 47	22 : 59
62	20 : 03	23 : 02
63	20 : 08	23 : 05
64	20 : 18	23 : 23
65	20 : 31	23 : 34

Table 6: The optimized dwelling times for each train (min).

Train no.	Stations								Total
	2	3	4	5	6	7	8	9	
1	0	0	0	3	0	4	4	6	17
2	2	0	2	3	0	4	3	0	14
3	3	2	6	0	2	0	0	0	13
4	5	3	6	2	0	0	5	0	21
5	0	2	0	0	4	5	4	6	21
6	0	0	0	0	3	0	5	0	7
7	0	0	6	3	0	0	3	3	15
8	0	0	0	0	0	4	0	0	4
9	0	0	0	4	0	0	0	2	7
10	0	0	5	6	0	5	4	0	20
11	0	4	0	3	3	0	4	0	13
12	4	0	0	5	0	5	3	0	17
13	2	0	0	4	0	0	3	0	10
14	0	0	5	0	5	2	0	0	12
15	0	0	2	0	4	3	3	2	14
16	0	0	0	0	0	3	4	0	7
17	0	2	0	5	0	4	0	0	12
18	0	0	0	0	0	0	5	0	5
19	0	5	6	2	4	0	5	0	22
20	3	3	0	0	5	4	0	4	19
21	0	2	0	0	0	2	5	0	10
22	2	0	3	6	3	3	0	5	22
23	2	3	0	5	0	0	0	0	10
24	0	3	5	0	5	4	6	0	22
25	3	0	0	0	2	0	0	6	11
26	0	0	0	3	0	0	4	0	8
27	0	6	0	0	0	0	2	0	8
28	0	3	4	4	0	4	0	2	17
29	0	0	5	0	0	0	3	3	11
30	4	0	6	6	0	0	0	0	15
31	4	2	0	6	4	0	4	0	20
32	6	3	4	0	0	0	2	4	19
33	0	0	3	5	0	0	0	0	8
34	3	0	0	4	3	2	0	0	12
35	0	4	4	4	3	3	0	5	22
36	0	0	0	4	5	6	0	0	15
37	0	0	0	0	4	6	0	0	10
38	0	0	0	0	3	3	0	3	8
39	5	0	0	2	0	4	0	5	16
40	0	0	2	0	4	0	0	0	6
41	0	5	3	0	3	0	2	0	14
42	0	5	6	5	0	3	0	0	18
43	5	0	0	0	0	0	0	6	11
44	0	3	4	5	0	0	0	4	16
45	0	0	6	0	3	4	6	0	18
46	0	0	0	0	3	6	4	4	17
47	4	0	4	0	3	0	4	0	15
48	0	3	0	0	4	0	4	0	11

Table 6: Continued.

Train no.	Stations								Total
	2	3	4	5	6	7	8	9	
49	0	0	2	3	2	0	3	5	15
50	0	5	5	0	0	2	2	5	19
51	0	2	0	6	0	3	0	0	11
52	0	4	0	4	0	0	0	0	8
53	4	0	2	6	5	0	0	0	17
54	5	5	0	0	4	4	0	5	24
55	0	6	0	0	0	0	0	0	6
56	0	4	0	0	6	0	0	0	10
57	2	6	4	0	0	6	0	6	24
58	0	0	0	3	5	3	2	3	17
59	4	0	3	4	0	4	0	0	14
60	0	5	0	2	2	0	5	2	17
61	0	0	0	3	6	6	0	6	20
62	0	5	0	0	4	2	0	0	11
63	3	0	0	2	4	0	0	0	9
64	0	0	3	4	3	0	4	0	13
65	0	0	5	0	0	5	0	4	14

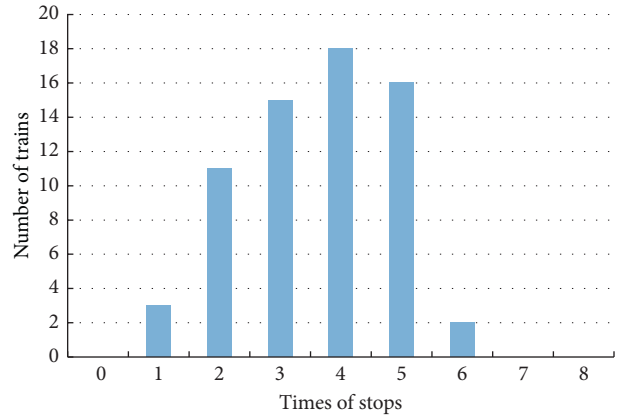

Figure 13: Times of train stopping at intermediate stations.

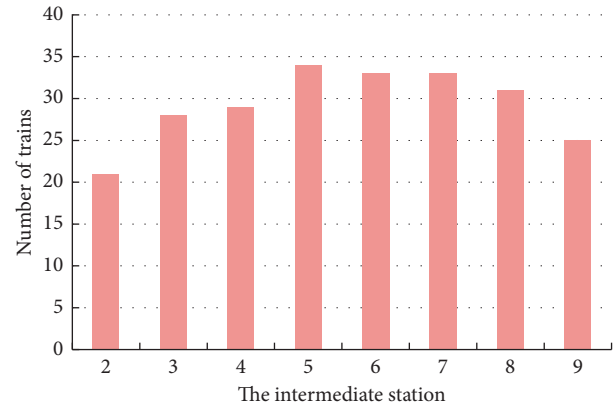

Figure 14: Number of trains stopping at intermediate stations.

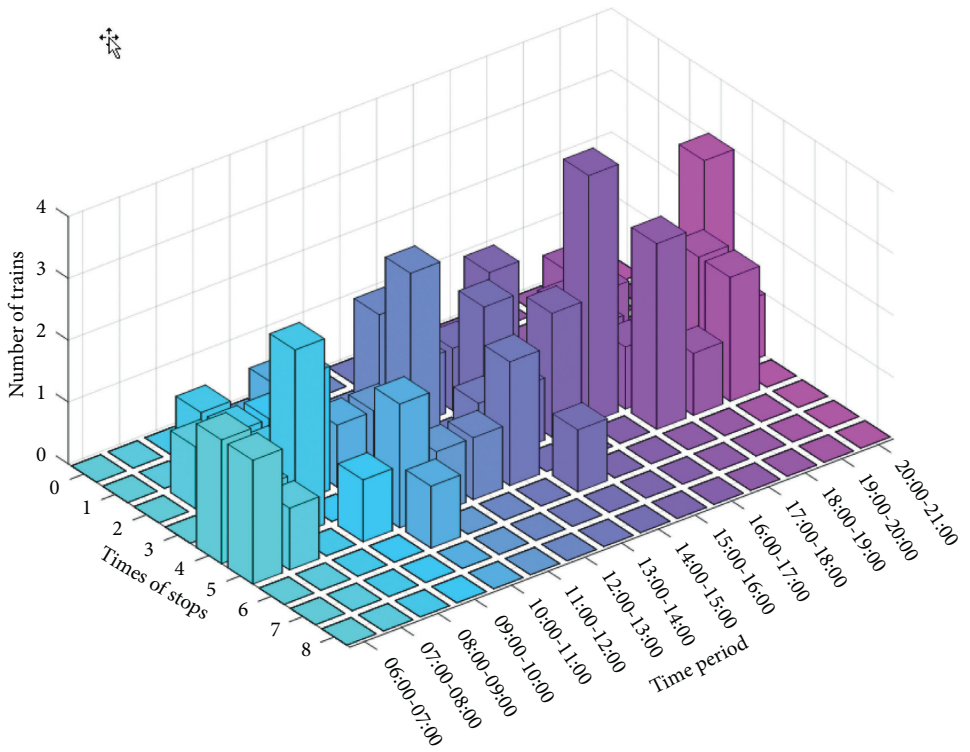

Figure 15: Number of trains with different number of stops in each period.

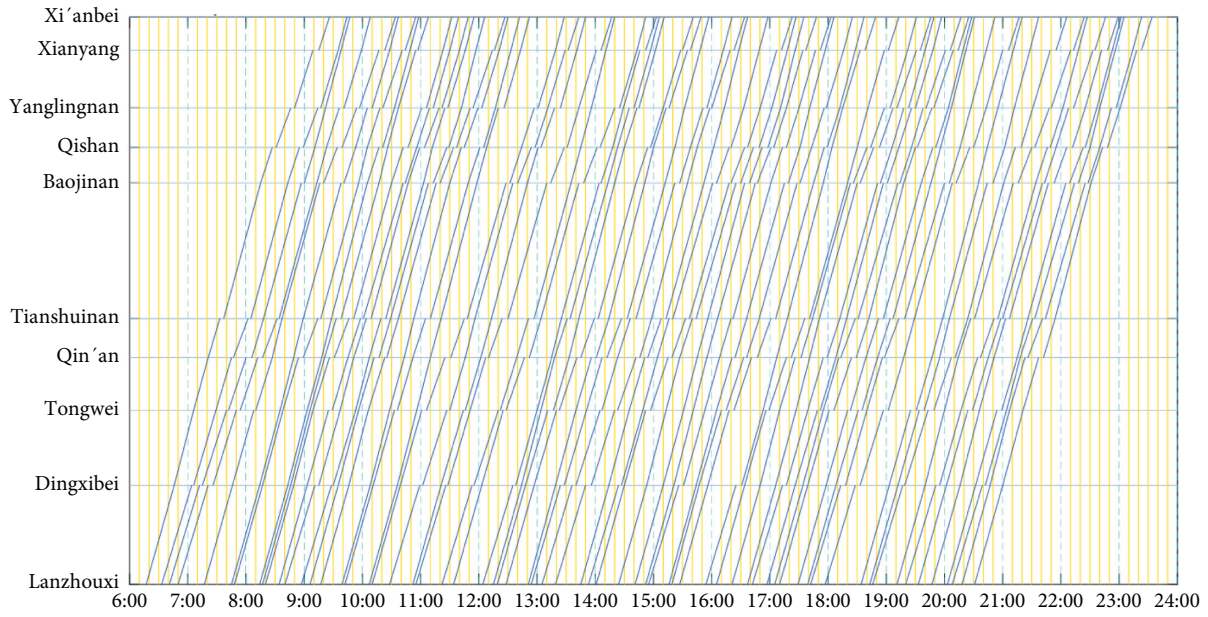

Figure 16: Train diagram based on optimized train timetable.

$P_m^2 = 0.05$, $P_m^3 = 0.03$, and maximum number of iterations to $Ge = 100$.

6.2. Computing Results. The departure time of all trains at initial station and the arrival time at terminal station are calculated, as shown in Table 5. In this scheme, the first train departs from the initial station at 6 : 17 and arrives at the terminal at 9 : 26. The last train departs from the departure station at 20 : 31 and arrives at the terminal station at 23 : 34. The optimized time horizon of train operation is basically consistent as the preplanned time horizon [6 : 00, 24 : 00].

The optimized skip-stop pattern and dwelling time of each train are shown in Table 6. The train with the least travel

Table 7: The number of passengers on each train (person).

Train no.	Passengers number
1	389
2	548
3	484
4	463
5	385
6	438
7	400
8	318
9	452
10	439
11	547
12	573
13	667
14	416
15	494
16	361
17	470
18	369
19	643
20	514
21	434
22	575
23	531
24	411
25	482
26	411
27	334
28	479
29	320
30	532
31	615
32	391
33	508
34	643
35	513
36	493
37	400
38	460
39	532
40	443
41	490
42	430
43	399
44	403
45	384
46	424
47	517
48	416
49	495
50	325
51	403
52	528
53	620
54	495
55	334
56	357
57	388
58	461
59	521
60	479
61	421
62	396
63	661
64	458
65	281

time is the 8th which dwells once at the intermediate station for 4 minutes; the trains with the longest travel time are the 22nd and 35th, which dwell 6 times, and the total dwelling time was 22 minutes.

The stopping times of different trains at intermediate stations are significantly different, as shown in Figure 13. In general, the number of trains dwelling at the intermediate station is relatively even, as shown in Figure 14, where there are more than 30 trains dwelling at intermediate stations 5, 6, 7, and 8, and more than 25 trains dwelling at intermediate stations 3, 4, and 9. There are also significant differences in the distribution of trains with different skip-stop pattern in each time period by hour, as shown in Figure 15.

By knowing the departure time of trains at initial station and the dwelling time at each intermediate station, an optimized train timetable can be derived, which is transformed into a graphical train timetable as shown in Figure 16. The number of passengers served by trains is shown in Table 7, where the 13th train served the most with a total of 667 passengers; the 65th train has the least number of passengers, 281; and the average value of trains service passengers is 461. The occupancy rate of a total of 65 trains in sections is shown in Figure 17.

Through calculation, passenger flow assignment results of a total of 45 OD pairs on trains can be obtained. The passengers' traveling information and the average value of generalized costs and are shown in Table 8. The time range of trains (from the earliest departure time to the latest departure time) that OD passengers can ride is 13 hours and 12 minutes on average. The smallest time range is that of OD pair (2,9), which is 8 hours and 17 minutes; the widest is that of OD pair (7,9) and (7,10), which is 14 hours and 17 minutes for both.

Passengers' generalized cost is the average of cost of the train they have taken, which meets the solving accuracy threshold of F–W algorithm in lower level model. Taking the OD pair (1,5) as an example, the number of trains that passengers can take is 34 trains, as shown in Table 9. The maximum and minimum generalized cost of trains with passenger loading are 120 and 106, respectively, as shown in Table 9.

Within the allowable error range, the passengers' generalized costs of the same OD pair are approximately equal as shown in Figure 18. From the analysis of the calculation results, it can be found that the unit impedance of most OD pairs is not very different, and only a few OD pairs have higher unit impedance, as shown in the figure for the 18th, 19th, 25th, 36th, 37th, 40th, 43rd, and 45th pairs. This is due to the difference in passenger departure time preferences

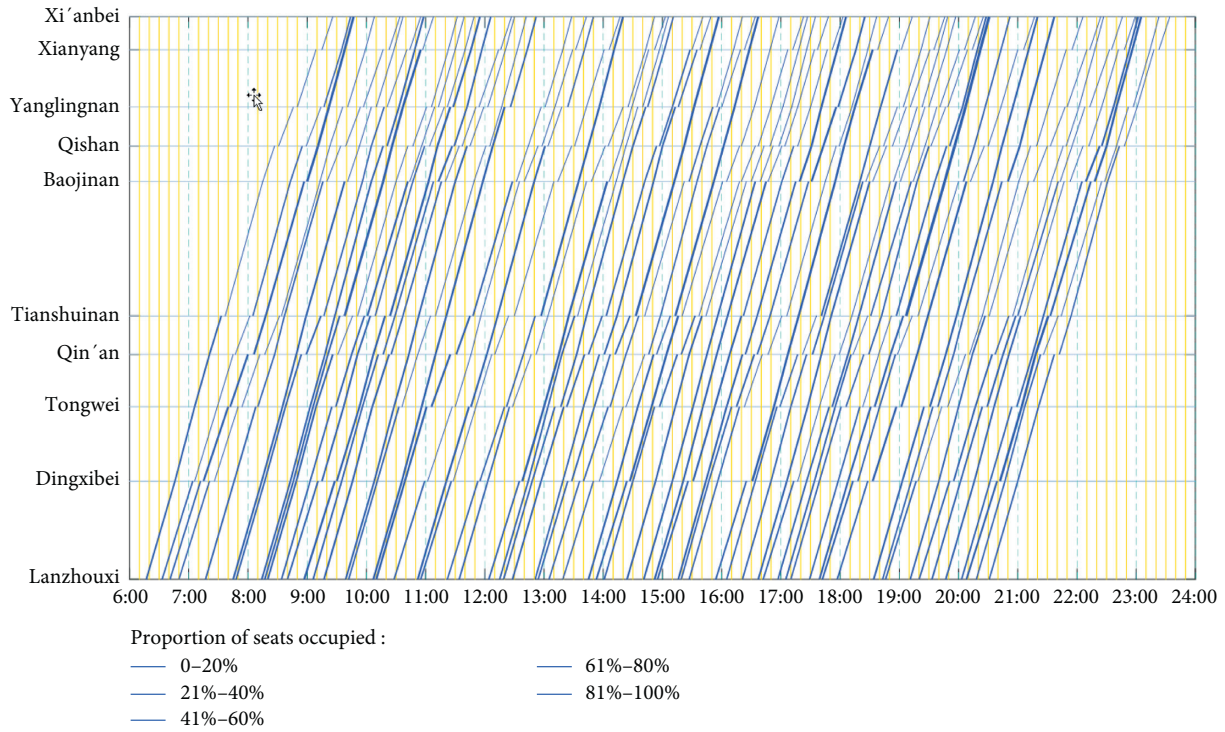

Figure 17: Train diagram with seats occupancy information.

Table 8: Departure time and travel generalized cost for each OD pairs.

OD pairs	Earliest departure time	Latest departure time	Number of trains	Generalized cost
1-2	6 : 33	20 : 08	21	41
1-3	6 : 41	20 : 03	28	73
1-4	6 : 33	20 : 18	29	94
1-5	6 : 17	20 : 18	34	114
1-6	6 : 41	20 : 18	33	164
1-7	6 : 17	20 : 31	33	182
1-8	6 : 17	20 : 18	31	200
1-9	6 : 17	20 : 31	35	226
1-10	6 : 17	20 : 31	65	239
2-3	7 : 15	19 : 19	8	34
2-4	7 : 06	19 : 55	10	59
2-5	7 : 06	20 : 42	13	76
2-6	7 : 15	20 : 42	10	125
2-7	7 : 06	19 : 55	9	145
2-8	7 : 06	17 : 17	7	163
2-9	11 : 02	19 : 19	8	186
2-10	7 : 06	20 : 42	21	200
3-4	7 : 42	19 : 49	12	33
3-5	7 : 54	20 : 29	13	48
3-6	7 : 42	20 : 59	14	99
3-7	8 : 10	20 : 59	13	118
3-8	7 : 54	20 : 29	13	134
3-9	8 : 10	20 : 29	10	160
3-10	7 : 42	20 : 59	28	176
4-5	7 : 47	21 : 26	16	23
4-6	8 : 06	21 : 26	14	77
4-7	7 : 47	21 : 42	14	97
4-8	7 : 47	21 : 26	15	113
4-9	8 : 59	21 : 42	12	141

Table 8: Continued.

OD pairs	Earliest departure time	Latest departure time	Number of trains	Generalized cost
4-10	7 : 47	21 : 42	29	150
5-6	10 : 01	21 : 44	14	59
5-7	7 : 37	21 : 07	16	77
5-8	7 : 37	21 : 44	15	97
5-9	7 : 37	21 : 07	12	120
5-10	7 : 37	21 : 44	34	135
6-7	9 : 20	22 : 09	17	25
6-8	9 : 20	22 : 28	16	44
6-9	9 : 20	21 : 53	13	67
6-10	9 : 00	22 : 28	33	80
7-8	8 : 31	21 : 33	13	22
7-9	8 : 31	22 : 48	16	50
7-10	8 : 31	22 : 48	33	59
8-9	8 : 50	22 : 13	11	31
8-10	8 : 50	22 : 57	31	43
9-10	9 : 15	23 : 23	25	19

Table 9: Departure/arrival time and travel generalized cost for OD pairs (1,5).

Train no.	Departure time	Arrival time	Passengers number	Generalized cost
1	6 : 17	7 : 33	173	110
2	6 : 33	8 : 02	0	130
4	6 : 50	8 : 32	0	129
7	7 : 48	9 : 14	142	116
9	8 : 17	9 : 33	0	134
10	8 : 20	9 : 46	171	108
11	8 : 34	9 : 58	50	110
12	8 : 40	10 : 04	142	118
13	8 : 57	10 : 19	93	118
17	9 : 42	11 : 05	162	106
19	10 : 10	11 : 45	137	118
22	10 : 55	12 : 24	0	135
23	11 : 22	12 : 51	0	132
26	12 : 15	13 : 31	256	109
28	12 : 28	13 : 59	104	118
30	12 : 54	14 : 27	0	129
31	13 : 05	14 : 36	134	116
33	13 : 45	15 : 08	0	127
34	13 : 53	15 : 16	268	111
35	14 : 01	15 : 33	86	116
36	14 : 24	15 : 40	297	115
39	14 : 55	16 : 20	134	120
42	15 : 27	17 : 01	114	117
44	16 : 05	17 : 36	0	125
49	17 : 05	18 : 28	0	129
51	17 : 29	18 : 52	0	127
52	17 : 39	19 : 04	0	128
53	17 : 42	19 : 13	80	111
58	19 : 11	20 : 27	267	109
59	19 : 20	20 : 51	137	113
60	19 : 33	20 : 58	142	118
61	19 : 47	21 : 03	291	115
63	20 : 8	21 : 31	153	111
64	20 : 18	21 : 41	61	117

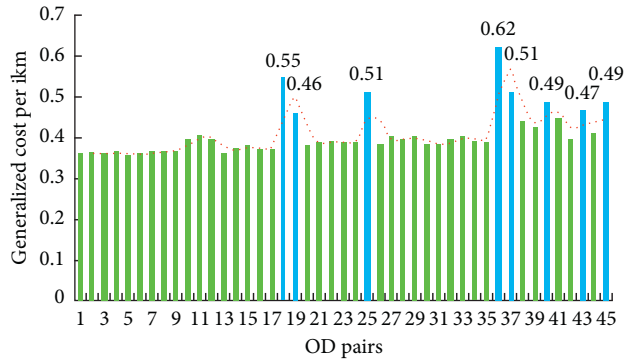

Figure 18: Generalized cost per kilometer for each OD pair.

between different OD pairs and the different service frequencies of trains at different stations.

7. Conclusions

In this paper, a high-speed railway (HSR) train timetable problem with passenger preferences is introduced; the specific conclusions are as follows:

(1) Passenger travel scheme and train timetable optimization are a set of dynamic game relationships. Constructing a bilevel programming model to specify the game process is proved to be effective by real-world example.

(2) It is a new method to transform the travel scheme selection of passengers into the path optimization problem in the space-time network, and it is proved to be an efficient method by numerical examples.

(3) The triangular fuzzy number method is used to quantify passengers' preference for departure time and analyze the reasons for the fluctuation of passenger flow. In this way, the generalized cost is established so that the train timetable can guide passengers to choose appropriate departure time, thereby reducing the waste of transportation capacity in certain time periods.

(4) Passengers travel according to the time period provided by an uneven train timetable, which satisfies the passenger flow assignment requirements mentioned in the first principle of Wardrop (user equilibrium).

The model and algorithm proposed in this paper provide an effective method for the train timetable that comprehensively considers the benefits of both service providers and passengers in a high-speed railway corridor. The train timetable optimization considering passenger transfer scheme on a complex high-speed railway network has not been studied, which is the direction of follow-up research.

Data Availability

The authors declare that the data used to support the findings of this study are real, and all authors are responsible for their originality. Besides, the data are included in the article and can be directly used by other authors who may need them.

Conflicts of Interest

The authors declare no conflicts of interest.

Acknowledgments

The work described in the paper was supported by National Natural Science Foundation of China (No. 71771109).

References

[1] X. Zhou and M. Zhong, "Single-track train timetabling with guaranteed optimality: branch-and-bound algorithms with enhanced lower bounds," *Transportation Research Part B: Methodological*, vol. 41, no. 3, pp. 320–341, 2007.

[2] B. P. Abbott, R. Abbott, T. D. Abbott et al., "Observation of gravitational waves from a binary black hole merger," *Physical Review Letters*, vol. 116, no. 6, Article ID 061102, 2016.

[3] H. Niu and X. Zhou, "Optimizing urban rail timetable under time-dependent demand and oversaturated conditions," *Transportation Research Part C: Emerging Technologies*, vol. 36, pp. 212–230, 2013.

[4] M. Chen and H. Niu, "Optimizing schedules of rail train circulations by tabu search algorithm," *Mathematical Problems in Engineering*, vol. 2013, no. 12, pp. 1–7, 2013.

[5] X. Xu, K. Li, L. Yang, and J. Ye, "Balanced train timetabling on a single-line railway with optimized velocity," *Applied Mathematical Modelling*, vol. 38, no. 3, pp. 894–909, 2014.

[6] M. Heydar, M. E. H. Petering, and D. R. Bergmann, "Mixed integer programming for minimizing the period of a cyclic railway timetable for a single track with two train types," *Computers & Industrial Engineering*, vol. 66, no. 1, pp. 171–185, 2013.

[7] L. Wang, Y. Qin, and J. Xu, "A fuzzy optimization model for high-speed railway timetable rescheduling," *Discrete Dynamics in Nature and Society*, vol. 2012, no. 11, 22 pages, Article ID 827073, 2012.

[8] V. Cacchiani, A. Caprara, and P. Toth, "A column generation approach to train timetabling on a corridor," *4OR*, vol. 6, no. 2, pp. 125–142, 2008.

[9] A. Caprara, M. Fischetti, and P. Toth, "Modeling and solving the train timetabling problem," *Operations Research*, vol. 50, no. 5, pp. 851–861, 2002.

[10] V. Cacchiani, F. Furini, and M. P. Kidd, "Approaches to a real-world train timetabling problem in a railway node," *Omega*, vol. 58, pp. 97–110, 2016.

[11] J. Yin, T. Tang, L. Yang, Z. Gao, and B. Ran, "Energy-efficient metro train rescheduling with uncertain time-variant passenger demands: an approximate dynamic programming approach," *Transportation Research Part B: Methodological*, vol. 91, pp. 178–210, 2016.

[12] B. He, R. Song, S. He, and Y. Xu, "High-speed rail train timetabling problem: a time-space network based method with an improved branch-and-price algorithm," *Mathematical Problems in Engineering*, vol. 2014, no. 1, pp. 1–15, 2014.

[13] J. Yin, L. Yang, T. Tang, Z. Gao, and B. Ran, "Dynamic passenger demand oriented metro train scheduling with energy-efficiency and waiting time minimization: mixed-integer linear programming approaches," *Transportation Research Part B: Methodological*, vol. 97, pp. 182–213, 2017.

[14] S. D. Gupta, J. K. Tobin, and L. Pavel, "A two-step linear programming model for energy-efficient timetables in metro railway networks," *Transportation Research Part B: Methodological*, vol. 93, pp. 57–74, 2016.

[15] H. Ye and R. Liu, "A multiphase optimal control method for multi-train control and scheduling on railway lines," *Transportation Research Part B: Methodological*, vol. 93, pp. 377–393, 2016.

[16] A. P. Cucala, A. Fernández, C. Sicre, and M. Domínguez, "Fuzzy optimal schedule of high speed train operation to minimize energy consumption with uncertain delays and driver's behavioral response," *Engineering Applications of Artificial Intelligence*, vol. 25, no. 8, pp. 1548–1557, 2012.

[17] S. Watanabe and T. Koseki, "Energy-saving train scheduling diagram for automatically operated electric railway," *Journal of Rail Transport Planning & Management*, vol. 5, no. 3, pp. 183–193, 2015.

[18] H. Niu, X. Zhou, and R. Gao, "Train scheduling for minimizing passenger waiting time with time-dependent demand and skip-stop patterns: nonlinear integer programming models with linear constraints," *Transportation Research Part B: Methodological*, vol. 76, pp. 117–135, 2015.

[19] E. Hassannayebi, S. H. Zegordi, and M. Yaghini, "Timetable optimization models and methods for minimizing passenger waiting time at public transit terminals," *Transportation Planning & Technology*, vol. 40, pp. 1–27, 2017.

[20] E. Hassannayebi, S. H. Zegordi, and M. Yaghini, "Train timetabling in urban rail transit line using Lagrangian relaxation approach," *Applied Mathematical Modelling*, vol. 40, no. 23-24, pp. 9892–9913, 2016.

[21] E. Barrena, D. Canca, L. C. Coelho, and G. Laporte, "Exact formulations and algorithm for the train timetabling problem with dynamic demand," *Computers & Operations Research*, vol. 44, no. 3, pp. 66–74, 2014.

[22] D. Canca, E. Barrena, A. De-Los-Santos, and J. L. Andrade-Pineda, "Setting lines frequency and capacity in dense railway rapid transit networks with simultaneous passenger assignment," *Transportation Research Part B: Methodological*, vol. 93, pp. 251–267, 2016.

[23] M. Shakibayifar, E. Hassannayebi, and H. Jafary, "Stochastic optimization of an urban rail timetable under time-dependent and uncertain demand," *Applied Stochastic Models in Business & Industry*, vol. 33, no. 6, 2017.

[24] X. Zhou and M. Zhong, "Bicriteria train scheduling for high-speed passenger railroad planning applications," *European Journal of Operational Research*, vol. 167, no. 3, pp. 752–771, 2005.

[25] J. Shi, L. Yang, J. Yang, and Z. Gao, "Service-oriented train timetabling with collaborative passenger flow control on an oversaturated metro line: an integer linear optimization approach," *Transportation Research Part B: Methodological*, vol. 110, pp. 26–59, 2018.

[26] T. Zhang, D. Li, and Y. Qiao, "Comprehensive optimization of urban rail transit timetable by minimizing total travel times under time-dependent passenger demand and congested conditions," *Applied Mathematical Modelling*, vol. 58, pp. 421–446, 2018.

[27] L. Kang, X. Zhu, H. Sun, J. Puchinger, M. Ruthmair, and B. Hu, "Modeling the first train timetabling problem with minimal missed trains and synchronization time differences in subway networks," *Transportation Research Part B: Methodological*, vol. 93, pp. 17–36, 2016.

[28] X. Guo, J. Wu, and H. Sun, "Timetable coordination of first trains in urban railway network: a case study of Beijing," *Applied Mathematical Modelling*, vol. 40, no. 17-18, pp. 8048–8066, 2016.

[29] R. C. W. Wong, T. W. Y. Yuen, K. W. Fung, and J. M. Y. Leung, "Optimizing timetable synchronization for rail mass transit," *Transportation Science*, vol. 42, no. 1, pp. 57–69, 2008.

[30] A. H. F. Chow and A. Pavlides, "Cost functions and multi-objective timetabling of mixed train services," *Transportation Research Part A: Policy and Practice*, vol. 113, pp. 335–356, 2018.

[31] O. J. Ibarra-Rojas, R. Giesen, and Y. A. Rios-Solis, "An integrated approach for timetabling and vehicle scheduling problems to analyze the trade-off between level of service and operating costs of transit networks," *Transportation Research Part B: Methodological*, vol. 70, no. 7, pp. 35–46, 2014.

[32] X. Li, D. Wang, K. Li, and Z. Gao, "A green train scheduling model and fuzzy multi-objective optimization algorithm," *Applied Mathematical Modelling*, vol. 37, no. 4, pp. 2063–2073, 2013.

[33] P. Mo, L. Yang, Y. Wang, and J. Qi, "A flexible metro train scheduling approach to minimize energy cost and passenger waiting time," *Computers & Industrial Engineering*, vol. 132, no. JUN, pp. 412–432, 2019.

[34] R. Liu, S. Li, and L. Yang, "Collaborative optimization for metro train scheduling and train connections combined with passenger flow control strategy," *Omega*, vol. 90, no. Jan., pp. 101990.1–101990.18, 2020.

[35] Y. Shen, G. Ren, and Y. Liu, "Timetable design for minimizing passenger travel time and congestion for a single metro line," *PROMET-Traffic&Transportation*, vol. 30, no. 1, p. 21, 2018.

[36] X. Tian and H. Niu, "A bi-objective model with sequential search algorithm for optimizing network-wide train timetables," *Computers & Industrial Engineering*, vol. 127, pp. 1259–1272, 2019.

[37] Y. Huang, L. Yang, T. Tang et al., "Saving energy and improving service quality: bicriteria train scheduling in urban rail transit systems," *IEEE Transactions on Intelligent Transportation Systems*, vol. 17, no. 12, pp. 1–16, 2016.

[38] Y. Zhu, B. Mao, Y. Bai, and S. Chen, "A bi-level model for single-line rail timetable design with consideration of demand and capacity," *Transportation Research Part C: Emerging Technologies*, vol. 85, pp. 211–233, 2017.

[39] Z. Huang and H. Niu, "A Bi-level programming model to optimize train operation based on satisfaction for an intercity rail line," *Discrete Dynamics in Nature and Society*, vol. 2014, Article ID 432096, 7 pages, 2014.

[40] J. Brimberg, E. Korach, M. Eben-Chaim et al., "The capacitated p-facility location problem on the real line," *International Transactions in Operational Research*, vol. 8, no. 6, pp. 727–738, 2010.

[41] L. Sun, J. G. Jin, D.-H. Lee, K. W. Axhausen, and A. Erath, "Demand-driven timetable design for metro services," *Transportation Research Part C: Emerging Technologies*, vol. 46, pp. 284–299, 2014.